Theoretical Study of Stable Trans and Cis Isomers in $[UO_2(OH)_4]^{2-}$ Using Relativistic Density Functional Theory

Georg Schreckenbach, P. Jeffrey Hay,* and Richard L. Martin

Theoretical Division (MS B268) and Seaborg Institute for Transactinium Science Los Alamos National Laboratory, Los Alamos, New Mexico 87545

Received January 20, 1998

The title compound, uranyl(VI) tetrahydroxide $[UO_2(OH)_4]^{2-}$, has been studied in detail using density functional theory (DFT) in the first systematic theoretical study of the compound. Scalar relativistic effects are included approximately by replacing the uranium core with a relativistic effective core potential. A total of nine stable structures have been characterized. Four of them (**I**−**IV**) possess the usual linear uranyl bond, and rapid exchange between these conformations is expected at finite temperatures. The uranyl and U−OH bond lengths of the minimum energy structure, **I**, are calculated as 1.842 and 2.334 Å, respectively. This compares well with the experimental crystal structure values of 1.824(3) Å and 2.258(3) Å, respectively. The existence of stable structures with a bent uranyl bond ("cis-uranyl") is predicted for the first time (structures **V**−**IX**). These conformers are only 18−19 kcal/mol higher in energy than the global energy minimum, and their uranyl bond angles cover a range of 113−132°. Harmonic vibrational frequencies for all stable conformers, **I**−**IX**, were calculated. They are compared to experiment where possible. A mechanism is suggested for the nonaqueous intramolecular oxygen ligand exchange in $[UO_2(OH)_4]^{2-}$ between uranyl and hydroxide involving a "cis-uranyl" structure as a stable intermediate in a two-step process with a calculated activation energy of 38 kcal/mol.

Introduction

Despite considerable progress over the past few years, the theoretical description of the chemistry of the f-block elements remains a considerable challenge.[1] There are at least three major problems that one must face in dealing with molecules containing heavy atoms. First, there is the large number of electrons, most of them occupying relatively inert core shells. Second, relativistic effects are crucial for even a qualitative understanding of the actinide compounds. Finally, correlation effects must be included to obtain reliable quantitative descriptions of molecular properties such as thermochemistries. Recent reviews by Pyykkö,[2] Pepper and Bursten,[3] and Almlöf and Gropen[4] have reviewed the available theoretical tools for relativistic quantum chemistry.

Because of their radioactivity, actinide complexes also present a challenge to experimental investigations. This presents an opportunity for theoretical studies to provide useful information on actinide molecular processes where experimental probes may be difficult to apply. The chemistry of uranium and other actinide elements in aqueous media has recently seen considerable interest experimentally,[5−8] motivated in large part by the desire to understand processes of environmental relevance such as reactions occurring in the groundwater at contaminated sites. Central to the aqueous chemistry of uranium and other actinide elements are their complexes with water and the hydroxide ion. For the higher valence states such as U(VI), a prominent role is played by the very stable uranyl UO_2^{2+} ions and their complexes.[9] We present in this contribution a detailed study of the title compound, uranyl tetrahydroxide, $[UO_2(OH)_4]^{2-}$. This compound has been found in alkaline solutions containing the uranyl ion UO_2^{2+} and has been characterized extensively in a recent study by Clark et al.[10] The experimental work provides information to help benchmark theoretical methods, and at the same time theory can provide additional insights into the chemistry of these actinide complexes.

Pepper and Bursten[3] have reviewed theoretical studies on actinide compounds including the uranyl species, and Denning has reviewed[9] the electronic structure, bonding, and spectroscopy of the uranyl ion UO_2^{2+}. Van Wezenbeek et al. have studied relativistic effects in UO_2^{2+} and UO_2.[11] Tatsumi and Hoffmann[12] and Wadt[13] have investigated why uranyl is linear in contrast to other MO_2^{2+} species on the basis of molecular orbital arguments. The uranyl unit has been found to be linear in all experimentally known complexes so far.

(1) Schreckenbach, G.; Hay, P. J.; Martin, R. L. *J. Comput. Chem.*, accepted.
(2) Pyykkö, P. *Chem. Rev.* **1988**, *88*, 563.
(3) Pepper, M.; Bursten, B. E. *Chem. Rev.* **1991**, *91*, 719.
(4) Almlöf, J.; Gropen, O. In *Reviews in Computational Chemistry*; Lipkowitz, K. B., Boyd, D. B., Eds.; Verlag Chemie: Weinheim, Germany, and New York, 1996; Vol. 8, p 203.
(5) Clark, D. L.; Hobart, D. E.; Neu, M. P. *Chem. Rev.* **1995**, *95*, 25.
(6) Katz, J. J.; Seaborg, G. T.; Morss, L. R. *The Chemistry of Actinide Elements*; Chapman and Hall: London, 1986.
(7) Grenthe, I.; Fuger, J.; Konings, R. J. M.; Lemire, R. J.; Muller, A. B.; Nguyen-Trung; Cregu, C.; Wanner, H. *Chemical Thermodynamics of Uranium*; Elsevier: Amsterdam, The Netherlands, 1992.
(8) Dozol, M.; Hagemann, R.; Hoffman, D. C.; Adloff, J. P.; von Gunten, H. R.; Foos, J.; Kasprzak, K. S.; Liu, Y. F.; Zvara, I.; Ache, H. J.; Das, H. A.; Hagemann, R. J. C.; Herrmann, G.; Karpol, P.; Maenhaut, W.; Nakahara, H.; Sakanoue, M.; Tetlow, J. A.; Baro, G. B.; Fardy, J. J.; Benes, P.; Roessler, K.; Roth, E.; Burger, K.; Steinnes, E.; Kostanski, M. J.; Peisach, M.; Liljenzin, J. O.; Aras, N. K.; Myasoedov, B. F.; Holden, N. E. *Pure Appl. Chem.* **1993**, *65*, 1081.
(9) Denning, R. G. *Struct. Bonding (Berlin)* **1992**, *79*, 215.
(10) Clark, D. L.; Conradson, S. D.; Donohoe, R. J.; Keogh, D. W.; Morris, D. E.; Palmer, P. D.; Rogers, R. D.; Tait, C. D. *Inorg. Chem.*, to be submitted.
(11) van Wezenbeek, E. M.; Baerends, E. J.; Snijders, J. G. *Theor. Chim. Acta* **1991**, *81*, 139.
(12) Tatsumi, K.; Hoffmann, R. *Inorg. Chem.* **1980**, *19*, 2656.
(13) Wadt, W. R. *J. Am. Chem. Soc.* **1981**, *103*, 6053.

S0020-1669(98)00057-3 CCC: $15.00
Published on Web 08/07/1998

The rich chemistry of uranyl complexes, which typically have several equatorial ligands bound to the UO_2^{2+} moiety, have received relatively little theoretical attention. Among the few recent studies[14−16] to date, Craw et al.[15] examined the structures of uranyl nitrate and sulfate complexes with Hartree−Fock calculations employing relativistic effective core potentials. To the best of our knowledge, there have been no previous theoretical studies of complexes between uranyl ions and water or hydroxide.

In the present study, various conformers and transition states of the uranyl tetrahydroxide ion, $[UO_2(OH)_4]^{2-}$, have been investigated theoretically. We use an approach in which scalar relativistic effects are incorporated by relativistic effective core potentials and correlation effects are included using density functional theory (DFT),[17,18] and in particular the hybrid B3LYP density functional.[19−22] Currently, DFT is one of the few first-principles methods that can treat large actinide complexes reasonably accurately. We were able to characterize a total of nine stable structures of the molecule, **I**−**IX**. Four of them, **I**−**IV**, have the usual linear uranyl bond. However, there are (at least) five possible stable conformers with a bent uranyl bond, **V**−**IX**, with uranyl bond angles of around 110° to about 130°, see below. These "cis-uranyl" structures are calculated to lie about 18−19 kcal/mol higher in energy than the ground state. This is the first evidence for the possibility of complexes with local minima corresponding to nonlinear uranyl units. These "cis-uranyl" structures also appear to play a particularly important role as intermediates in ligand exchange processes of the uranyl tetrahydroxide, as we discuss below. While the structures with bent uranyl units represent local minima, rather than the global minimum for $[UO_2(OH)_4]^{2-}$, the current results open the possibility of detecting these metastable species experimentally for the current case of OH ligands and the intriguing option of stabilizing the cis structure as the ground state with other ligand sets.

We have further calculated the transition states that connect several of the stable structures. We have finally considered possible reaction mechanisms for the intramolecular oxygen exchange[10] between uranyl oxygens and hydroxide oxygens. We propose an intramolecular mechanism that could occur in nonaqueous media for this process that involves some of the "cis-uranyl" structures as stable intermediates. In addition, possibilities of intermolecular solvent-assisted exchange reactions in water are discussed briefly.

Theoretical Approach and Computational Details

We use density functional theory (DFT)[17,18,23,24] for our calculations. In the past few years, DFT has been recognized as an efficient and remarkably accurate means of treating electron correlation effects in molecules. It is therefore particularly powerful for metal complexes and other large systems. We chose the B3LYP hybrid density functional[19−22,25] out of the various possible choices for the exchange-correlation density functional. This approach has recently gained popularity since it seems to be capable of reproducing accurate geometries and thermochemistries among other properties[26,27] not only of the first-row compounds, to which it was originally fitted, but also of transition metal complexes.[28−30]

We reduce the number of variational electrons and include relativistic effects by using a relativistic effective core potential (ECP)[31] for uranium. The uranium core comprises the electrons in all shells up to and including the $4f^{14}$ and $5d^{10}$ shells leaving the outer $6s^2$ $6p^6$ and the outer six valence electrons (5f, 6d, 7s, 7p) treated explicitly. The uranium ECP has been derived from a Hartree−Fock (HF) relativistic atomic calculation. Experience to date[32,33] suggests that HF-derived ECPs can be transferred to DFT calculations, although this issue is not altogether resolved. We also neglect spin−orbit effects, which are typically less important in the ground state of closed-shell systems[34,35] that we are considering here.

We use the GAUSSIAN94 program package[36] for the calculations that are reported in this contribution. A locally modifed version of the GAUSSIAN94 program package[30] is employed to obtain analytic first and second derivatives of the total energy with respect to nuclear displacement. Such derivatives are essential to optimize geometries and to calculate vibrational frequencies.

We apply the following basis sets, unless otherwise stated: On uranium, a general ECP valence basis set[31] is employed in its completely uncontracted version. On the oxygen and hydrogen atoms, the standard 6-31+G* all-electron basis sets are used.[37] For a more detailed discussion of the basis set requirements, see Appendix: Basis Sets.

Achieving SCF convergence is problematic for these actinide complexes, but a procedure of "building the guess" has been reasonably successful. In short, for any given structure, one starts at the HF level of theory with a minimal basis set. The converged set of molecular orbitals (MO) forms the input for the next calculation, using an increased basis set, and so on, until the desired level of theory is reached. At some intermediate level of basis set, one should use the converged HF-SCF results as input for a DFT calculation with the same basis set. "Level shifting" of virtual MOs is also useful to reach convergence at any given intermediate level. Thus, for a given basis set level, one single-point calculation is done including level shifting. This is always followed by another single-point SCF run without level shifting, before going on to the next higher basis sets. Geometry optimizations and frequency calculations are always done without any level shifting.

Results and Discussion

Stable "Trans" Structures of $[UO_2(OH)_4]^{2-}$. As mentioned in the Introduction, we have investigated various stable con-

(14) Pyykkö, P.; Li, J.; Runeberg, N. *J. Phys. Chem.* **1994**, *98*, 4809.
(15) Craw, J. S.; Vincent, M. A.; Hillier, I. H.; Wallwork, A. L. *J. Phys. Chem.* **1995**, *99*, 10181.
(16) Oda, Y.; Funasaka, H.; Nakamura, Y.; Adachi, H. *J. Alloys Compd.* **1997**, *255*, 24.
(17) Parr, R. G.; Yang, W. *Density-Functional Theory of Atoms and Molecules*; Oxford University Press: New York, Oxford, 1989.
(18) Ziegler, T. *Chem. Rev.* **1991**, *91*, 651.
(19) Lee, C.; Yang, W.; Parr, R. G. *Phys. Rev. B* **1988**, *37*, 785.
(20) Becke, A. D. *J. Chem. Phys.* **1993**, *98*, 5648.
(21) Stephens, P. J.; Devlin, F. J.; Chabalowski, C. F.; Frisch, M. J. *J. Phys. Chem.* **1994**, *98*, 11623.
(22) Becke, A. D. In *Modern Electronic Structure Theory, Part II*; Yarkony, D. R., Ed.; World Scientific: Singapore, 1995; p 1022.
(23) Ziegler, T. *Can. J. Chem.* **1995**, *73*, 743.
(24) Bartolotti, L. J.; Flurchick, K. In *Reviews in Computational Chemistry*; Libkowitz, K. B., Boyd, D. B., Eds.; Verlag Chemie: Weinheim, Germany, and New York, 1995; Vol. 7, p 187.
(25) Vosko, S. H.; Wilk, L.; Nusair, M. *Can. J. Phys.* **1980**, *58*, 1200.
(26) Cheeseman, J. R.; Trucks, G. W.; Keith, T. A.; Frisch, M. J. *J. Chem. Phys.* **1996**, *104*, 5497.
(27) Bühl, M. *Chem. Phys. Lett.* **1997**, *267*, 251.
(28) Ricca, A.; Bauschlicher, C. W. *Theor. Chim. Acta* **1995**, *92*, 123.
(29) Ricca, A.; Bauschlicher, C. W. *J. Phys. Chem.* **1995**, *99*, 9003.
(30) Russo, T. V.; Martin, R. L.; Hay, P. J.; Rappé, A. K. *J. Chem. Phys.* **1995**, *102*, 9315.
(31) Hay, P. J. *J. Chem. Phys.* **1983**, *79*, 5469.
(32) Russo, T. V.; Martin, R. L.; Hay, P. J. *J. Phys. Chem.* **1995**, *99*, 17085.
(33) van Wüllen, C. *Int. J. Quantum Chem.* **1997**, *58*, 147.
(34) van Lenthe, E. Ph.D. Thesis, Free University, Amsterdam, The Netherlands, 1996.
(35) van Lenthe, E.; Snijders, J. G.; Baerends, E. J. *J. Chem. Phys.* **1996**, *105*, 6505.
(36) Frisch, M. J.; Trucks, G. W.; Schlegel, H. B.; Gill, P. M. W.; Johnson, B. G.; Robb, M. A.; Cheeseman, J. R.; Keith, T.; Petersson, G. A.; Montgomery, J. A.; Raghavachari, K.; Al-Laham, M. A.; Zakrzewski, V. G.; Ortiz, J. V.; Foresman, J. B.; Cioslowski, J.; Stefanov, B. B.; Nanayakkara, A.; Challacombe, M.; Peng, C. Y.; Ayala, P. Y.; Chen, W.; Wong, M. W.; Andres, J. L.; Replogle, E. S.; Gomperts, R.; Martin, R. L.; Fox, D. J.; Binkley, J. S.; Defrees, D. J.; Baker, J.; Stewart, J. P.; Head-Gordon, M.; Gonzalez, C.; Pople, J. A. *Gaussian 94*, Revision E.1; Gaussian, Inc.: Pittsburgh, PA, 1995.
(37) Hehre, W. J.; Radom, L.; Schleyer, P. v. R.; Pople, J. A. *Ab Initio Molecular Orbital Theory*; John Wiley & Sons: New York, 1986.

Table 1. Calculated Energies and Calculated and Experimental Key Structural Parameters of the Stable "Trans-Uranyl" Conformers **I**−**IV** that Possess a Linear Uranyl Bond

struct	symmetry	energy[a] (kcal/mol)	bond lengths (Å)	
			uranyl	U−OH
I ("trans 2 up, 2 down")	D_{2d}	0	1.842	2.334
II ("cis 2 up, 2 down")	C_{2h}	0.1	1.843	2.333
III ("3 up, 1 down")	C_s	0.5	1.849, 1.836	2.336, 2.336 2.332, 2.333
IV ("all up")	C_{4v}	1.4	1.857, 1.829	2.335
exptl[b]			1.824 (av) [1.801(6)−1.835(5)]	2.250 (av) [2.229(5)−2.275(5)]
cryst struct[c]				
soln (EXAFS)			1.80(1)	2.21(1)[d]

[a] Relative to **I**. [b] Reference 10. [c] Crystal structure of $[Co(NH_3)_6]_2\,[UO_2(OH)_4]_3 \cdot 2H_2O$. [d] See the text for a discussion of the equatorial coordination number.

formations of $[UO_2(OH)_4]^{2-}$. The first four of them, **I**−**IV**, correspond to structures possessing the usual linear uranyl bond.

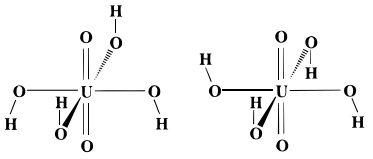

I **II**

They differ only by their arrangement of the terminal OH groups. Total energies and key geometry parameters are given in Table 1. While all of these structures are very close in energy, we predict that **I**, the "trans 2 up, 2 down" conformer, is the global energy minimum. The prediction is based on steric considerations and on the relativistic DFT/ECP calculations, Table 1. The experimental geometry[10] of $[UO_2(OH)_4]^{2-}$ has been obtained in aqueous solution and from the X-ray structure of $[Co(NH_3)_6]_2[UO_2(OH)_4]_3 \cdot 2H_2O$. The calculated uranyl bond length, 1.842 Å for **I**, is about 0.02 Å too long compared to the average experimental value from the crystal structure, 1.824(3) Å,[10] Table 1. The calculated U−OH bond lengths are generally too long by about 0.08 Å compared to the crystal structure.

In Table 1 the U−O bond distances as determined from EXAFS spectroscopy in solution are also shown. The first coordination shell was fitted with two O atoms at a U═O distance of 1.80 Å, slightly smaller than the average value of 1.824 Å in the crystal structure. The best fit for the U−O(H) bond distance corresponding to the second coordination shell of O atoms was 2.21 Å, also slightly smaller than the average value of 2.250 Å in the crystal structure. An accurate determination of the number of O(H) atoms in the second shell has proven more difficult. The most recent work,[10] completed since the original submission of this paper, leads to the interpretation that both $[UO_2(OH)_4]^{2-}$ and $[UO_2(OH)_5]^{3-}$ are present in solution, with the latter species as the dominant one. Similarly the best fit to the solution EXAFS data is obtained with approximately five O atoms in the second shell. In this paper the theoretical calculations will focus on the tetrahydroxide species, and consideration of pentahydroxide and other species with higher coordination numbers will be addressed in future publications.

The experimental crystal structure contains three independent $[UO_2(OH)_4]^{2-}$ ions in the unit cell, and the corresponding uranyl bond distances span a range from 1.801(6) to 1.835(5) Å.[10] The three independent $[UO_2(OH)_4]^{2-}$ ions per unit cell might correspond to more than one structure out of structures **I**−**IV**. For example, one of the uranyl tetraoxide ions shows two different values for the uranyl bond distance, $R(U{=}O_1) = 1.801(6)$ Å and $R(U{=}O_2) = 1.829(6)$ Å, respectively.[10] This particular ion could therefore correspond to the C_{4v} "all up" structure **IV**; note the difference between $R(U{=}O_2)$ and $R(U{=}O_1)$ of about 0.03 Å, which compares favorably to the calculated numbers for **IV**, Table 1. Further, all four experimental U−OH bond distances are almost identical for this ion at 2.270(4) and 2.261(5) Å, respectively. The other two uranyl ions in the crystal structure have in either case identical uranyl bond distances, of 1.835(5) and 1.823(5) Å, respectively. Hence, they could, at least approximately, correspond to structure **I** or **II**. The actual hydrogen positions have not been resolved in the crystal structure, and no clear conclusion is possible regarding the conformers. It should also be noted that Clark et al.[10] attributed the different uranyl bond lengths to varying amounts of hydrogen bonding in the crystal structure.

Table 2. Calculated Total Energies and Key Structural Parameters of the Stable "Cis-Uranyl" Conformers **V**−**IX**

struct	energy[a] (kcal/mol)	bond lengths (Å)		uranyl bond angle (deg)
		uranyl	U−OH	
V	18.0	1.874, 1.870	2.267, 2.320 2.349, 2.349	128.4
VI	19.2	1.899, 1.899	2.252, 2.252 2.346, 2.346	112.7
VII	19.3	1.910, 1.888	2.257, 2.244 2.349, 2.349	114.0
VIII	18.5	1.862, 1.880	2.268, 2.326 2.348, 2.353	129.4
IX	19.3	1.847, 1.891	2.268, 2.336 2.354, 2.354	131.6

[a] Relative to **I**.

Stable "Cis" Structures of $[UO_2(OH)_4]^{2-}$. Properties of another set of stable structures of $[UO_2(OH)_4]^{2-}$ have been collected in Table 2. These conformations (structures **V**−**IX**)

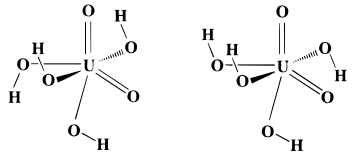

V **VI**

are shown in Figure 1 with their optimized structures. The structures are unusual because they are predicted to possess a bent uranyl bond; the bond angles range from 113° to 132°. The "cis-uranyl" structures are higher in energy then the linear uranyl structures by 18−19 kcal/mol, Table 2, depending on the hydrogen arrangement. Nevertheless, on the basis of geometry optimizations and calculated harmonic frequencies, we predict these conformations to be stable, i.e., they correspond to local minima on the potential energy surface. The uranyl

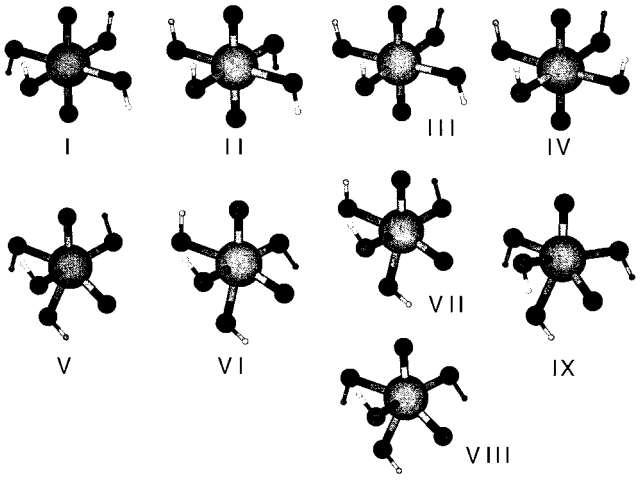

Figure 1. Perspective pictures for the optimized structures of the stable conformations **I**−**IX**.

Table 3. Calculated Charges[a] at the Different Nuclei for the "Trans" Structure **I**, as Well as for the "Cis" Structure **V**

	charge (au)	
nucleus	**I**	**V**
U	2.42	2.30
O[b]	−0.90	−0.87
O(H)[c]	−1.06	−1.03 to −1.07
H	0.41	0.40 to 0.46

[a] From Mulliken population analysis. [b] Uranyl oxygens. [c] Hydroxide oxygens.

bond is computed to be longer in these structures, by about 0.04−0.06 Å. This is remarkable since the measured uranyl bond length of 1.824 Å (for the conformers with a linear uranyl bond) is already considered to be unusually long.[10] The U−OH bond lengths span a fairly wide range in structures **V**−**IX**; the variations seem to be caused by steric effects.

Electronic Structure and Bonding. In this section we discuss briefly the electronic structure of the uranyl tetrahydroxide species using the charge distribution and molecular orbitals from our B3LYP hybrid density functional calculations.[19−22] The primary emphasis will be on examination of the orbital character of the occupied and low-lying virtual orbitals in terms of the participation of the ligand and U valence 6d, 5f, 7s, and 7p orbitals. We will be less concerned with making quantitative correlations with experiment since (a) the physical significance of the ground state molecular orbitals for the singly ionized molecule or of virtual orbitals for excited states is not justified in density functional theory and (b) the fact that the molecular species is a dianion with no counterions results in numerous occupied (as well as virtual) orbitals with positive energies.

The overall charge distribution is summarized in Table 3, where the calculated charges from Mulliken population analysis are given for "trans" and "cis" $[UO_2(OH)_4]^{2-}$ (structures **I** and **V**). A rather ionic picture, with a calculated charge of +2.42 and +2.30 on the uranium in the "trans" and "cis" species, respectively, is given by the Mulliken analysis. Starting from a +6 formal valence, the charge of +2.42 in **I** indicates a net valence population of 3.58e in the outer uranium orbitals, which are apportioned as 1.05e from 6d and 2.68e from the 5f component, of which the largest contribution (1.20e) comes from the $5f_0$ atomic orbital. Only qualitative meaning should be assigned to these Mulliken values, since this analysis gives a total population in s and p orbitals on the U of 7.85e, which is 0.15e less than the 8.0e in the $6s^2$ $6p^6$ "outer core" electrons.

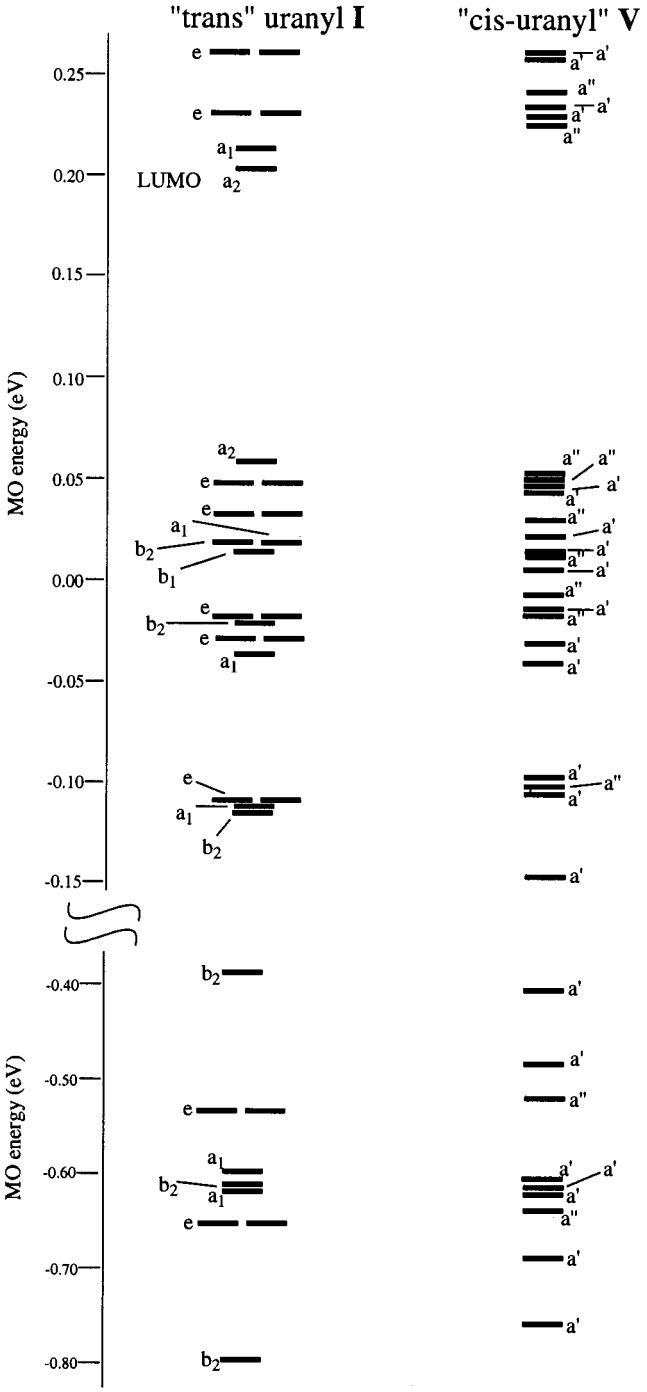

Figure 2. MO energy level diagram for structures **I** ("trans-uranyl", D_{2d} symmetry) and **V** ("cis-uranyl", C_s symmetry). The MO energy levels are taken from the B3LYP-DFT calculations; valence-occupied MOs as well as a few virtual MOs are shown. Note the different energy scales in the upper and lower parts of the diagram.

For the "cis" compound **V** the total populations are as follows: 1.03 6d, 2.80 5f, and 7.83 in s plus p.

The calculated orbital energies in the "trans" and "cis" forms of uranyl tetrahydroxide are shown in Figure 2, where the orbitals are labeled by their respective symmetries in the D_{2d} ("trans" structure **I**) and C_s ("cis" structure **V**) point groups of the molecules. In Table 4 the orbitals are compared in more detail, and the major atomic components of each molecular orbital in the "trans" form **I** are also given. In the "trans" form the O═U═O axis lies along the *z*-axis with the U−OH bonds oriented along *x* and *y*. In the "cis" form, which is not analyzed in detail in the table, the bent O═U═O species lies in the *xz*-

Table 4. MO Symmetry Labels, Calculated MO Energies, and Major Orbital Character for Structures **I** (Trans) and **V** (Cis)

MO no.[a]	sym label ("trans")[b]	"trans" MO energy[b] (eV)	major orbital character [minor components][d] for "trans" [b]	sym label ("cis")[c]	"cis" MO energy[c] (eV)
8	b_2	−0.793	O 2s + U $6p_z$	a′	−0.756
9	e	−0.650	O_H 2s + U $6p_{x,y}$	a′	−0.687
10	e	−0.650	O_H 2s + U $6p_{x,y}$	a″	−0.636
11	a_1	−0.611	O 2s + U 6s	a′	−0.619
12	b_2	−0.610	O_H 2_s	a′	−0.612
13	a_1	−0.595	O_H 2_s	a′	−0.603
14	e	−0.531	O_H 2s − U $6p_{x,y}$	a″	−0.517
15	e	−0.531	O_H 2s − U $6p_{x,y}$	a′	−0.481
16	b_2	−0.385	O 2s − U $6p_z$	a′	−0.404
17	b_2	−0.114	O_H − H σ bond	a′	−0.144
18	a_1	−0.111	O_H − H σ bond	a′	−0.103
19	e	−0.108	O_H − H σ bond	a″	−0.100
20	e	−0.108	O_H − H σ bond	a′	−0.095
21	a_1	−0.036	O $2p_z$ + U 7s	a′	−0.039
22	e	−0.027	O $2p_{x,y}$ [+U $5f_\pi$, $6d_\pi$]	a′	−0.029
23	e	−0.027	O $2p_{x,y}$ [+U $5f_\pi$, $6d_\pi$]	a″	−0.015
24	b_2	−0.020	O $2p_z$ [+U $7p_z$]	a′	−0.014
25	e	−0.017	O $2p_{x,y}$	a″	−0.005
26	e	−0.017	O $2p_{x,y}$	a′	0.007
27	b_1	0.016	O_H $2p_{lone}$	a″	0.013
28	a_1	0.016	O_H $2p_\sigma$ [+U 7s]	a′	0.015
29	b_2	0.017	O_H $2p_\sigma$ [+U $5f_\sigma$, $7p_\sigma$]	a′	0.023
30	e	0.034	O_H $2p_{lone}$ [+U $5f_\phi$]	a″	0.031
31	e	0.034	O_H $2p_{lone}$ [+U $5f_\phi$]	a′	0.046
32	e	0.049	O_H $2p_{lone}$ [+U $7p_\pi$]	a′	0.051
33	e	0.049	O_H $2p_{lone}$ [+U $7p_\pi$]	a″	0.052
34 (HOMO)	a_2	0.059	O_H $2p_{lone}$	a″	0.052
35 (LUMO)	a_2	0.204	U $5f_\delta$	a″	0.226
36	a_1	0.214	U $5f_\delta$	a′	0.231
37	e	0.231	U $5f_\phi$	a′	0.235
38	e	0.231	U $5f_\phi$	a″	0.243
39	e	0.265	U $6p_\pi$	a′	0.260
40	e	0.265	U $6p_\pi$	a′	0.264

[a] MOs are counted with increasing MO energy, for the actual calculations that replaced the uranium core with an ECP (cf. Theoretical Approach and Computational Details). [b] Structure **I** of D_{2d} symmetry. [c] Structure **V** of C_s symmetry. Note that orbitals are listed in eigenvalue order and do not necessarily correlate with the same orbitals from the "trans" structure. [d] O and O_H refer to the oxygen atoms of U═O and U−OH, respectively.

plane. Since the occupied orbitals, aside from the "outer core" 6s and 6p shells on U, are ligand in character, the minor contributions from the metal are indicated in brackets in the table.

The bonding in the uranyl ion $(UO_2)^{2+}$ has been the subject of numerous studies.[9,12,13] Because these treatments have tended to emphasize the splitting of the 5f manifold in the axial field and to minimize somewhat the interactions with the equatorial ligands, it is worthwhile to review briefly the nature of the 5f orbitals. We shall deal with the combinations of the original complex spherical harmonics which produce real functions as follows:

$5f_0$	$5f_\sigma$	$2z^3 - 3z(x^2 + y^2)$
$5f_{\pm1}$	$5f_\pi$	$2xz^2 - x^3 - xy^2$
		$2yz^2 - y^3 - yx^2$
$5f_{\pm2}$	$5f_\delta$	$z(x^2 - y^2)$
		$2xyz$
$5f_{\pm3}$	$5f_\varphi$	$x^3 - 3xy^2$
		$3x^2y - y^3$

where the angular functions are not normalized and the radial portions, represented by Gaussian functions, are also not included. According to their angular properties the $5f_0$ and $5f_{\pm1}$ orbitals contribute to σ and π bonds, respectively, and have a_1 and e symmetry in the D_{2d} point group of the "trans" structure **I**. The $5f_\delta$ and $5f_\varphi$ orbitals have δ and φ bonding character about the O═U═O axis with the former having e symmetry and the latter transforming as a_1 and a_2 in D_{2d}.

As shown in Figure 2, the occupied orbitals of $[UO_2(OH)_4]^{2-}$ are roughly organized into four groups according to orbital energies. Not shown in the figure are the U 6s and O 1s core orbitals. At lowest energies are the orbitals arising from U 6p and O 2s orbitals. There is considerable interaction in this group, especially between the U $6p_z$ orbital and the antisymmetric O 2s combination on the axial O atoms of the U═O bonds leading to stabilization of the $1b_2$ MO and destabilization of the $3b_2$ MO. This interaction was emphasized by Tatsumi and Hoffmann[12] in their extended Hückel analysis of uranyl bonding with a linear UO_2^{2+} group as contrasted to bent ThO_2 and other group 4 transition metal dioxides. They argued that increased $5f_0$ participation in the bonding led to stabilization of the linear O═U═O linkage and that this participation was induced by interactions with the high-lying $3b_2$ orbital arising from interactions involving the "outer core" U 6p and O 2s orbitals. Ab initio Hartree−Fock calculations using relativistic ECPs by Wadt[13] gave the correct linear and bent structures for UO_2^{2+} and ThO_2, respectively. His analysis accounted for linear structure for UO_2^{2+} from the dominant interactions with the 5f orbitals which are lower than the 6d orbitals, while in ThO_2 one has the ordering 6d < 5f and the 6d orbitals stabilize the bent geometry in that case.

The next group of orbitals (17−20) constitute the O−H σ bonds of the hydroxide ligands. At somewhat higher energies are a group of six orbitals (21−26) essentially comprising the σ and π bonds of the O═U═O moiety. For the σ bond there are some U 7s participation in the a_1 orbital and U $7p_z$ contribution in the b_2 orbital of this group. Also there is some small admixture of $6d_\pi$ (*xz*, *yz*) and $5f_\pi$, reflecting some double-bond character.

Table 5. Calculated Harmonic Frequencies (cm^{-1}) (IR Intensities (km/mol) in Parentheses) of the "Trans-Uranyl" Conformer **I** (Global Energy Minimum) and the "Cis-Uranyl" Conformer **V**[a]

resonance no.	sym label for **I**[b]	**I**	**V**
1	E	90 (16)	59 (5)
2	E	90 (16)	103 (0)
3	B_1	99 (0)	127 (1)
4	A_1	112 (0)	149 (10)
5	B_2	161 (17)	163 (43)
6	E	168 (32)	214 (22)
7	E	168 (32)	239 (24)
8	A_2	221 (0)	252 (1)
9	E	248 (0)	266 (0)
10	E	248 (0)	328 (51)
11	B_1	271 (0)	334 (43)
12	E	290 (24)	334 (16)
13	E	290 (24)	370 (447)
14	B_2	319 (0)	378 (0)
15	E	370 (500)	379 (57)
16	E	370 (500)	425 (284)
17	A_1	383 (0)	539 (55)
18	B_2	585 (33)	623 (140)
19	E	591 (186)	632 (193)
20	E	591 (186)	660 (153)
21	A_1	599 (0)	709 (178)
22	A_1[c]	739 (0)	734 (223)
23	B_2[d]	823 (512)	875 (84)
24	E	3745 (5)	3687 (11)
25	E	3745 (5)	3733 (3)
26	A_1	3745 (0)	3734 (0)
27	B_2	3745 (0)	3790 (4)

[a] The symmetry labels refer to **I** only. [b] D_{2d} symmetry. [c] Symmetric uranyl stretch. [d] Antisymmetric uranyl stretch.

At slightly higher energies we find the group of eight orbitals (27−34) arising from the lone-pair orbitals on the equatorial O atoms of the OH ligands. They basically separate into two groups of four. One set is composed of the lone pairs that are perpendicular to the U−O−H plane, which are denoted as $2p_{lone}$ in the table. The second set is composed of lone pairs that point toward the U forming the U−OH σ bonds, denoted as $2p_\sigma$ in the table. The $2p_\sigma$ set produces MOs of a_1, b_2, and e symmetry, while the $2p_{lone}$ set gives rise to MOs of b_1, a_2, and e symmetry. In these orbitals there is a slight amount of $5f_\sigma$ admixture in the a_1 U−OH σ bonding orbital, and there is some $5f_\phi$ admixture in the e combination of the lone pairs.

The first four virtual orbitals correspond to the U $5f_\delta$ (a_1, a_2) and $5f_\varphi$ (e) orbitals, respectively. These are the familiar lowest lying orbitals in analyses of the UO_2^{2+} ion, which in weakly interacting environments typically are closely spaced but have the reverse ordering $5f_\varphi < 5f_\delta$. The next virtual orbitals arise from the U 7p (e) set. We re-emphasize that little quantitative value should be placed on the actual orbital energies since they are taken from a ground state density functional for a molecule with an overall charge of −2.

Vibrational Frequencies. Calculated harmonic vibrational frequencies and infrared (IR) intensities have been collected in Table 5 for the "trans-uranyl" conformer **I** (global energy minimum) and the corresponding "cis-uranyl" conformer **V** as obtained from analytic second derivatives calculated at the respective minimum energy geomtries of each species. Table 6 contains the calculated uranyl stretching frequencies ν_1 and ν_2 of all the "trans-uranyl" structures **I**−**IV**. Additional calculated vibrational frequencies and IR intensities for all stable structures are listed in the Supporting Information. While Raman intensities would also be a useful tool, this involves the calculation of third derivatives of the total energy.[38]

Experimental data[10] exists only for the uranyl stretching frequencies on which we will concentrate in the following. The other frequencies have been included into Table 5 and the Supporting Information for reference. The calculated uranyl stretching frequencies ν_1 and ν_2 are very close between the different "linear uranyl" conformers **I**−**IV**, Table 6. This is not too surprising since structures **I**−**IV** differ primarily by their arrangement of the terminal hydrogen atoms, which should not influence the central O═U═O unit too strongly. In particular, the calculated uranyl bond lengths are fairly similar for all four structures, Table 1.

Table 6. Calculated (for the "Trans-Uranyl" Conformers **I**−**IV**) and Experimental Uranyl Stretching Frequencies ν_1 and ν_2

	uranyl stretch (cm^{-1})	
conformer	sym, ν_1	asym, ν_2
I	739	823
II	737	822
III	738	824
IV	735	826
expt		
single cryst[a]	796	
soln[a]	784, 786[b]	

[a] Reference 10. [b] The number depends on other ions that may be present in the solution.

Experimental data exists for the symmetric frequency ν_1 which is Raman active. The Raman spectrum of solid $[Co(NH_3)_6]_2[UO_2(OH)_4]_3 \cdot 2H_2O$ (single crystals) shows a peak at 796 cm^{-1}. The experimentally obtained frequency is, in solution, 784 or 786 cm^{-1}, respectively, depending on the other ions that may be present in the solution.[10] Clark et al. note that this is the lowest symmetric uranyl stretching frequency that has been reported in the literature so far. The calculated ν_1 frequencies are even smaller by about 45−50 cm^{-1} (Tables 5 and 6), a significant deviation from experiment. The harmonic frequencies have been calculated at the equilibrium geometry in each case. Earlier, we discussed that the calculated uranyl bond lengths are too long by about 0.02 Å. It is well-known that theoretical vibrational frequencies are very sensitive to the reference geometry[39−44] as well as to the type of functional used in the DFT calculation. To calculate the harmonic frequencies at some reference point other then a stationary point on the potential energy surface would require dealing with the nonzero forces at such a point. We speculate that part of the discrepancy can be attributed to the overestimate of the bond length by the B3LYP hybrid functional, and that frequency calculations at the experimental geometry would improve the agreement with the experimental spectra.

Transition States between "Trans " and "Cis" Uranyl Structures. A number of transition states have been characterized by calculations of their electronic structure and geometry. The nature of the stationary point has been confirmed in every case by calculating the vibrational frequencies, thus confirming that exactly one frequency is imaginary. The different transition state structures are shown schematically in Figure 3. Their optimized geometries are displayed in Figure 4, and the total energies are summarized in Table 7. The table contains further

(38) Frisch, M. J.; Yamaguchi, Y.; Schaefer, H. F., III; Binkley, J. S. *J. Chem. Phys.* **1986**, *84*, 531.
(39) Pulay, P.; Fogarasi, G.; F., P.; Boggs, J. E. *J. Am. Chem. Soc.* **1979**, *101*, 2550.
(40) Fogarasi, G.; Zhou, X. F.; Taylor, P. W.; Pulay, P. *J. Am. Chem. Soc.* **1992**, *114*, 8191.
(41) Bérces, A. Ph.D. Thesis, University of Calgary, Calgary, Alberta, Canada, 1995.
(42) Bérces, A.; Ziegler, T. *J. Phys. Chem.* **1995**, *99*, 11417.
(43) Bérces, A. *J. Phys. Chem.* **1996**, *100*, 16538.
(44) Bérces, A.; Ziegler, T. *Top. Curr. Chem.* **1996**, *182*, 41.

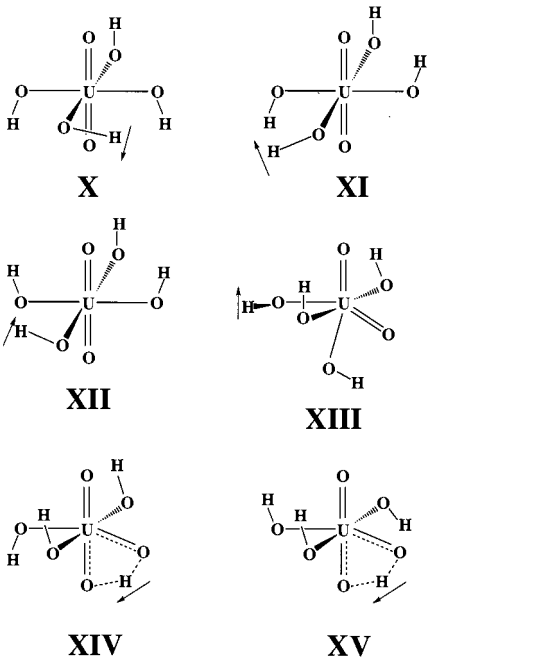

Figure 3. Schematic representation of the various transition states, structures **X**−**XV**. The most important process, i.e., the hydrogen movement at the transition state, has been marked with an arrow in every case.

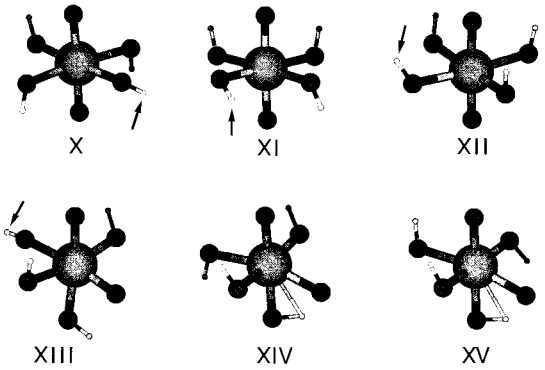

Figure 4. Perspective pictures for the optimized structures of the various transition states, structures **X**−**XV**. Note that the actual bonding in **XIV** and **XV** is better represented by the schematic structures of Figure 3. The moving proton is marked by an arrow in structures **X**−**XIII**.

the calculated imaginary frequency that identifies a given transition state. This frequency characterizes the local curvature of the potential energy surface in the vicinity of the transition state, for small displacements along the reaction coordinate.

We would like to start with transition states that connect the stable structures with linear uranyl bonds, **I**−**IV**, with the newly predicted "cis-uranyl" conformers that possess a bent uranyl bond, **V**−**IX**. We have characterized two transition states of this sort. Thus, the transition state **XIV**, calculated (at the given level of theory) at an energy of 38.7 kcal/mol above the minimum energy conformation **I**, is the transition state for the intramolecular hydrogen rearrangement between **I** and **V**. Likewise, **XV** represents the transition state, at 37.6 kcal/mol above the global energy minimum, between the "cis 2 up, 2 down" conformer **II** and the corresponding "cis-uranyl" structure **VI**, Table 7. Similar transition states between the "3 up, 1 down" conformer **III** and the corresponding "cis-uranyl" structures **VII** and **VIII**, as well as between the C_{4v} structure **IV** and its counterpart **IX**, could certainly be determined.

Table 7. Calculated Energies[a] and Imaginary Transition Frequencies of Some Transition States, Structures **X**−**XV**

struct	energy of the transition state[a] (kcal/mol)	reactant (energy[a] (kcal/mol))	product (energy[a] (kcal/mol))	transition freq[b] (cm^{-1})
		"Cis" to "Trans" Pathways		
XIV	38.7	**I** (0.0)	**V** (18.0)	1707i
XV	37.6	**II** (0.1)	**VI** (19.2)	1687i
		"Trans" to "Trans" Pathway		
XVI[c]	58.7[c]	**II** (0.1)	**II** (0.1)	1619i,[c] 1715i[c]
		"Hydrogen Flip" Isomerizations		
X	0.7	**I** (0.0)	**III** (0.5)	136i
XI	0.8	**II** (0.1)	**III** (0.5)	130i
XII	1.5	**III** (0.5)	**IV** (1.4)	130i
XIII	20.7	**V** (18.0)	**VII** (19.3)	134i

[a] Relative to **I**. [b] A true transition state is always characterized by one imaginary frequency, corresponding to the reaction coordinate in the vicinity of the transition state. This frequency is given here. [c] Calculated at the lower contracted/6-31G basis set level, see the text. **XVI** is not a true transition state since it has two imaginary frequencies.

Hydrogen Flip Transition States. Another set of transition states, structures **X**−**XIII**, have been characterized as well, cf. Table 7 and Figures 3 and 4. These are transition states for the exchange between the different stable conformers of $[UO_2(OH)_4]^{2-}$.

Structures **X**−**XII** represent the transition states that correspond to hydrogen flips between the various stable conformers with linear uranyl bonds, Figure 3. These reactions occur by a rotation of one OH group around its U−OH bond. The activation energy is very low (well below 1 kcal/mol) in every case, Table 7. Therefore, there will be rapid exchange between the different structures **I**−**IV**. Rapid interchange is also possible between the various "cis-uranyl" structures, structures **V**−**IX**. As an example, we have studied the interchange between structures **V** and **VII**. The transition state, **XIII**, is in this case 1.4 kcal/mol higher in energy than the product, **VII**, and 2.7 kcal/mol higher in energy than the reactant, **V**, Table 7.

In this connection, it is also interesting to consider a hypothetical uranyl tetrahydroxide structure of D_{4h} symmetry, i.e., with a planar $U(OH)_4$ arrangement that is perpendicular to the O═U═O uranyl axis. This structure is predicted to have a total of eight imaginary frequencies (eighth-order saddle point), and it has an energy of 28.2 kcal/mol as compared to **I**. The eight imaginary frequencies correspond to hydrogen movements in a plane perpendicular to the respective U−O bond vector, which can be related to the optimized transition states for the hydrogen flip, **X**−**XII**.

Intramolecular Oxygen Exchange. In their recent study Clark et al.[10] found experimental evidence for rapid uranyl oxo ligand exchange in highly alkaline $[UO_2(OH)_4]^{2-}$ solutions. Evidence for this exchange process was provided by line-width resonance analysis, which showed broadening when the temperature was raised from 25 to 94 °C. This behavior was opposite to what was found in acid media, where no exchange is known to occur, and the ^{17}O uranyl line width sharpened with increasing temperature. On the basis of the line-width analysis they derived activation parameters for this process, for which a barrier height of $\Delta H^{\ddagger} = 9.8 \pm 0.7$ kcal/mol was determined. Finally samples prepared using ^{18}O-enriched water in alkaline solution showed a new feature at 752 cm^{-1} compared to the ^{16}O uranyl Raman frequency of 784 cm^{-1}. Upon redissolution into $H_2{}^{16}O$, the 752 cm^{-1} feature was reduced, and the 784 cm^{-1} feature grew.

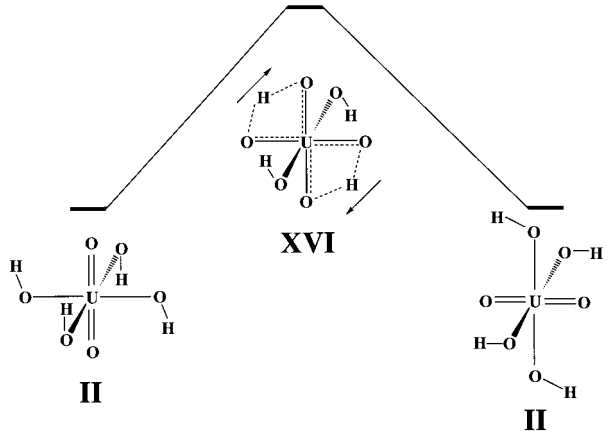

Figure 5. Intramolecular ligand exchange in $[UO_2(OH)_4]^{2-}$: schematic representation of a hypothetical concerted hydrogen rearrangement reaction. Note that the intermediate structure, **XVI**, is not a true transition state since it has two imaginary frequencies (see the text for details).

It is interesting to investigate whether theory is capable of reproducing these experimental results, while presumably providing insight into the reaction mechanism. Clark et al.[10] have also investigated the hydroxide ion exchange in solution. However, this process is beyond the scope of the present paper. We will come back to the experiments of Clark et al. again later.

Possibly the most obvious and appealing mechanism would include some kind of concerted transition state that connects, for instance, the "cis 2 up, 2 down" conformer **II** with itself. This hypothetical process is shown schematically in Figure 5. A systematic study of this reaction reveals that it cannot be the lowest energy pathway for the ligand exchange. Thus, we attempted to optimize the geometry of the transition state structure **XVI**. At a lower level of theory (contracted basis on U, 6-31G basis for the ligands), a stationary point was found. It had an energy of 58.6 kcal/mol compared to the reactant and product **II**. However, the structure, **XVI**, has two imaginary frequencies, Table 7. This proves that **XVI** is not a true transition state but rather a second-order saddle point on the potential energy surface. One of the two imaginary frequencies corresponds to the desired concerted hydrogen rearrangement while the other one has the two hydrogens move in the same direction. Similar imaginary frequencies were calculated for **XVI** at the higher level of theory (uncontracted basis on U, 6-31+G* basis for the ligands, see above). However, **XVI** is probably not a stationary point at this level of theory, and attempts to optimize its geometry failed consistently.

The failure of the concerted hydrogen rearrangement led us to propose another mechanism for the intramolecular ligand exchange in the uranyl tetrahydroxide ion. The process avoids the concerted hydrogen movement and is demonstrated in Figure 6. It involves as a stable intermediate the "cis-uranyl" structure **VI** (19.1 kcal/mol higher in energy than reactant and product). The transition state is **XV**, which has an energy of 37.5 kcal/mol compared to **II**, and of 18.4 kcal/mol compared to **VI**, Figure 6. The process involves a successive proton movement. Starting from **II**, one proton moves via a transition state, **XV**, to form the stable intermediate, **VI**, with a "cis-uranyl" arrangement. From there, a second proton is moved. In this manner, the product, **II**, is reached, again via a transition state, **XV**. Thus, uranyl oxygens can exchange with hydroxide oxygens through an intramolecular process, Figure 6.

It should be noted that one could construct a completely similar reaction profile with the "3 up, 1 down" conformer **III** as reactant and product, and with the corresponding "cis-uranyl" structure **VII** as the stable intermediate. The activation energy for this process should be comparable in magnitude. Further, one could also construct a reaction profile involving the global energy minimum, **I**, and the corresponding "cis-uranyl" structure **V**. The transition state **XIV** connects those two structures, as has been pointed out before. However, to complete the oxygen exchange between uranyl and hydroxide oxygens, some isomerization of the intermediate structure **V** would be required. This could, for instance, involve the transition state **XIII** that connects **V** with **VII**, see above. It is clear, then, that the proposed process as outlined in Figure 6 is only one out of several possible reaction pathways for the intramolecular oxygen exchange in uranyl tetrahydroxide.

We are now at the point to return to the experimentally determined oxo ligand exchange. Clark et al.[10] conclude that the observed ligand exchange is water facilitated with an activation energy of $\Delta H^{\ddagger} = 9.8 \pm 0.7$ kcal/mol, see above. It is obvious, then, that our proposed mechanism cannot be compared directly with the experimental result since we have not considered water explicitly. Our mechanism would apply to nonaqueous solutions where the ligand exchange rate is known to be considerably lower than in the aqueous media. In aqueous solutions one can, however, envisage a similar mechanism involving the conversion of the "trans" to "cis" isomers assisted by a solvent water in which proton transfer from the water to the uranyl oxygen of the "trans" isomer produces the "cis" isomer. This hypothetical reaction is shown schematically in Scheme 1a.

In a subsequent step another water molecule carries out a similar process regenerating the "trans" isomer, but with uranyl and hydroxide oxygens exchanged, Scheme 1b.

This stepwise process would involve the exchange of two protons with the solvent water molecules. The uranyl oxygens are exchanged with hydroxide oxygens in the product **II** as compared to the reactant in Scheme 1a. Elucidation of these solvent-assisted pathways will require further theoretical and experimental investigation to determine the reaction intermediates in these processes.

Conclusion

The present paper constitutes the first systematic study of the uranyl tetrahydroxide ion, $[UO_2(OH)_4]^{2-}$, and one of the few theoretical studies on uranyl complexes reported to date. A major goal of the study was to further test the accuracy and feasibility of applying relativistic ECPs[31] within the framework of DFT. At this point, we are able to conclude that relativistic DFT, using the B3LYP hybrid functional,[19-22] is capable of quantitative predictions about the structure and vibrational frequencies of actinide complexes.

We were able to characterize a number of stable conformers for $[UO_2(OH)_4]^{2-}$. These include the structures **V**−**IX** that are predicted to possess a nonlinear uranyl bond. Given that these structures are only 18−19 kcal/mol higher in energy than the ground state, it might become possible to synthesize uranyl complexes with a "cis" arrangement of the uranyl units. In their experimental paper, Clark et al.[10] discuss the unusually long uranyl bond in conjunction with the low uranyl stretching frequency ν_1. Both observations point to a weak uranyl bond in this particular complex. Clark et al. argue that the OH^- ligands are strong π-donors. Partial π-bonding along the U−OH bonds in the equatorial plane of the molecule would be in competition with the uranyl bonds, and it could explain the comparatively long and weak U═O bonds. Clark et al. base

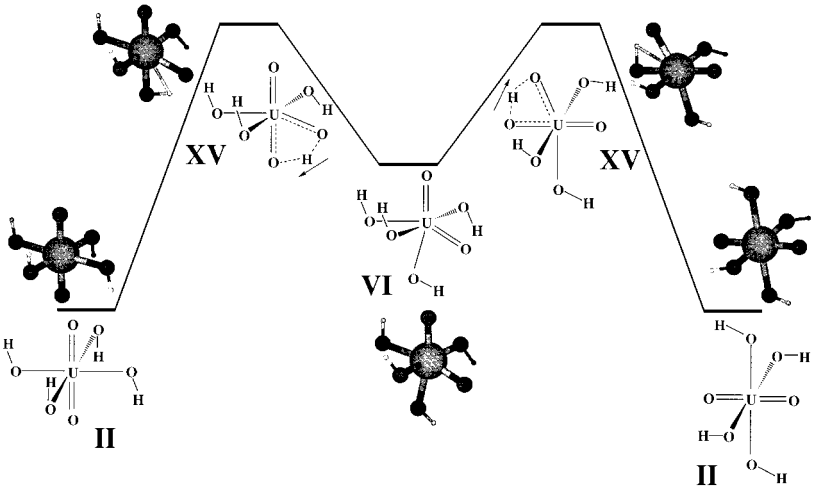

Figure 6. Nonaqueous intramolecular ligand exchange in $[UO_2(OH)_4]^{2-}$. The transition state, **XV**, and the intermediate "cis-uranyl" structure, **VI**, are calculated to have total energies relative to **II** of 37.5 and 19.1 kcal/mol, respectively. The uranyl oxygens are exchanged with hydroxide oxygens in the product, as compared to the reactant.

Scheme 1

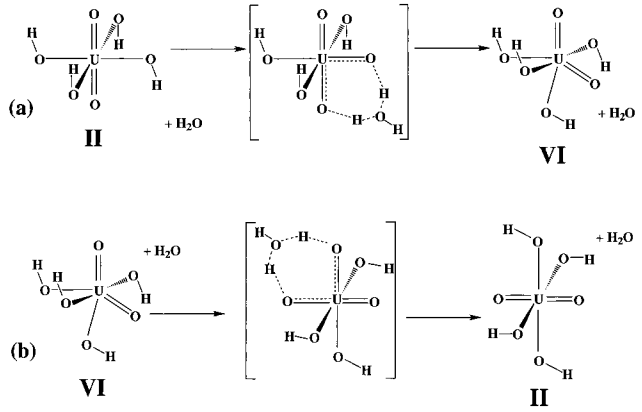

their arguments on an assumed D_{4h} symmetry for $[UO_2(OH)_4]^{2-}$. However, a similar argument can be applied to the actual conformations that possess lower symmetry (D_{2d}, C_{2h}, C_s, and C_{4v}, respectively, Table 1) and U−O−H bond angles of about 106°.

One would anticipate that "cis" O═An═O structures will arise in other actinyl species besides $[UO_2(OH)_4]^{2-}$. In fact, recent calculations by the authors[1] have found stable "cis" and "trans" isomers also in $[UO_2F_4]^{2-}$ and $[UO_2Cl_4]^{2-}$. One would also expect that the pentahydroxide uranyl species, which were inferred to exist in solution by EXAFS studies, could have isomers corresponding to linear and bent ("cis") uranyl structures.

We have proposed a reaction pathway, including the transition state, for the intramolecular oxygen exchange in uranyl tetrahydroxide, Figure 6. The proposed, nonconcerted pathway excludes the solvent explicitly, as has been discussed above; we have shown that a hypothetical concerted mechanism cannot be the minimum energy path. A "cis-uranyl" structure occurs as the stable intermediate in the proposed reaction. The experimental data points to a water-assisted reaction pathway in aqueous solution. It includes proton transfer from free water to the oxo groups and a corresponding proton transfer from a hydroxide group to the H_2O, "all of which may or may not be concerted." [10] Hence, a direct comparison between theory and experiment is not possible at the moment. It is, however, likely that the water-assisted transition state will proceed along a pathway that includes a "cis-uranyl" structure as a stable intermediate, in analogy to the nonaqueous pathway of Figure 6. Thus, the water-assisted pathway would not be concerted either, as has been shown schematically in Scheme 1. This assumption is further supported by the fact that solvation in a polar solvent (like water) will stabilize structures with a permanent dipole moment more than those without. Calculated dipole moments are given in Table 8 for structures **I**−**IX**. Of the "linear uranyl" structures, **I** and **II** have no permanent dipole moment, due to symmetry, while **III** and **IV** have a permanent dipole moment. Given the rapid exchange between the linear uranyl conformers **I**−**IV**, see above, it can be assumed that the average dipole moment of linear $[UO_2(OH)_4]^{2-}$ is small. All of the bent uranyl conformers, **V**−**IX**, have, on the other hand, a permanent dipole moment, and stabilizing solvent interactions should be present. To conclude, we could expect a polar solvent to stabilize the "cis-uranyl" conformers **V**−**IX** as compared to the "trans-uranyl" (linear-uranyl) ground state. Further studies are in progress or planned that shall address the importance of solvation effects and study the water-assisted ligand exchange in more detail.

Table 8. Calculated Electric Dipole Moments of the Stable Conformers **I**−**IX**

	I	**II**	**III**	**IV**	**V**	**VI**	**VII**	**VIII**	**IX**
calcd dipole moment (D)	0	0	2.09	3.71	0.92	1.19	1.98	2.05	3.58

Table 9. Influence of the Basis Set on the Optimized Geometry of the Minimum Energy Structure I ("Trans 2 Up, 2 Down") of $[UO_2(OH)_4]^{2-}$

	bond lengths (Å)		
basis set[a]	uranyl	U−OH	OH bond length (Å)
6-31G/contracted	1.8739	2.3056	0.9824
6-31G*/contracted	1.8556	2.3106	0.9710
6-31G/uncontracted	1.8688	2.3046	0.9821
6-31G*/uncontracted	1.8472	2.3133	0.9709
6-31G**/uncontracted	1.8463	2.3132	0.9673
6-31+G/uncontracted	1.8629	2.3212	0.9779
6-31+G*/uncontracted	1.8421	2.3338	0.9702
6-31++G*/uncontracted	1.8418	2.3338	0.9705
6-31+G**/uncontracted	1.8412	2.3341	0.9659
expt[b]	1.824(3)	2.258(3)	

[a] HF-derived ECP and contracted or uncontracted valence basis on uranium;[31] standard all-electron basis sets (6-31G etc.) on the ligands,[37] see the text. [b] Experimental data according to ref 10: crystal structure of $[Co(NH_3)_6]_2$ $[UO_2(OH)_4]_3 \cdot 2H_2O$.

Table 10. Influence of the Basis Set on the Energy and Optimized Geometry of a "Cis-Uranyl" Structure (**V**) of $[UO_2(OH)_4]^{2-}$

		bond lengths (Å)		
basis set[a]	total energy (kcal/mol) [b]	uranyl	U−OH	uranyl bond angle (deg)
6-31G/contracted	16.03	1.9048, 1.9024	2.2919, 2.2527 2.3146, 2.3146	125.5
6-31G*/contracted	17.54	1.8840, 1.8823	2.2984, 2.2486 2.3223, 2.3223	127.5
6-31G/uncontracted	17.08	1.9047, 1.9024	2.2809, 2.2510 2.3111, 2.3111	122.5
6-31G*/uncontracted	18.06	1.8798, 1.8777	2.2960, 2.2505 2.3212, 2.3212	126.2
6-31G**/uncontracted	18.49	1.8795, 1.8783	2.2929, 2.2512 2.3215, 2.3215	125.5
6-31+G/uncontracted	17.34	1.9051, 1.9001	2.2939, 2.2622 2.3320, 2.3320	122.2
6-31+G*/uncontracted	17.95	1.8745, 1.8700	2.3197, 2.2672 2.3489, 2.3489	128.4
6-31++G*/uncontracted	17.99	1.8734, 1.8691	2.3212, 2.2681 2.3496, 2.3496	128.9
6-31+G**/uncontracted	18.38	1.8759, 1.8721	2.3129, 2.2663 2.3496, 2.3496	126.8

[a] HF-derived ECP and contracted or uncontracted valence basis on uranium;[31] standard all-electron basis sets (6-31G etc.) on the ligands,[37] see the text. [b] Relative to the global minimum energy structure (at the same level of theory).

Acknowledgment. This work has been funded by the Laboratory Directed Research and Development program of the Los Alamos National Laboratory, operated by the University of California under contract to the U.S. Department of Energy. This work has been done in affiliation with the Seaborg Institute for Transactinium Science. The authors are grateful to our colleagues D. L. Clark and D.W. Keogh for inspiring discussions and for drawing our attention to the given subject. The optimized structures have been drawn with the MOLDEN freeware program.

Supporting Information Available: Tables 11 and 12 containing the calculated harmonic vibrational frequencies of all of the stable conformers, structures **I**−**IX** (4 pages). Ordering information is given on any current masthead page.

Appendix: Basis Sets

It is well-known that the choice of basis sets is important for reliable results. The computational effort is, on the other hand, proportional to some power of the number of basis functions. Hence, a good compromise between accuracy and efficiency has to be found for any given problem. We investigate the influence of the basis sets by studying two stable conformations of uranyl tetrahydroxide, $[UO_2(OH)_4]^{2-}$, Tables 9 and 10. Table 9 contains geometry parameters for the global minimum structure, **I**; Table 10 lists key geometry parameters and the total energy (taken relative to conformer **I**) for a stable "cis-uranyl" structure, **V**. On the uranium center, we use either a contracted valence basis set[31] or the same set but completely uncontracted. At the ligand atoms oxygen and hydrogen, we employ the standard all-electron 6-31G basis, possibly augmented with polarization functions (6-31G*, 6-31G**), with diffuse functions (6-31+G), or with a combination thereof (6-31+G*, 6-31++G*, and 6-31+G**).[37]

First, let us consider the relative energy between **I** and **V**, Table 10. The influence of the basis sets on this parameter is seen to be modest: the different basis sets result in variations of 2.5 kcal/mol or less. The polarization functions on the oxygen atoms (6-31G* basis) result in changes of 1.5 and 1 kcal/mol (for the contracted and uncontracted uranium basis sets, respectively). Diffuse functions (6-31+G etc.) and polarization functions on the hydrogen atoms (6-31G**) show less influence on the energy. Uncontracting the uranium basis yields changes of 1 and 0.5 kcal/mol (with the 6-31G and 6-31G* ligand basis sets, respectively).

The different basis sets have a strong influence on the optimized geometries of the uranyl tetrahydroxide conformers, Tables 9 and 10. The addition of polarization functions on the oxygen atoms (6-31G* vs 6-31G) has the most pronounced effect. It results in a contraction of the U═O double bond lengths of about 0.02 Å, and a lengthening of the U−OH bonds by 0.005−0.007 Å (structure **I**) and up to 0.01 Å (structure **V**), respectively. The oxygen polarization functions result in contractions of the O−H bonds by 0.005−0.007 Å, Table 9. The further addition of polarization functions to the hydrogen basis sets (basis 6-31G**) yields, however, only small changes in the optimized bond lengths, even for the O−H bond lengths (0.004 Å in this case).

Uncontracting the uranium basis is seen to be important as well, although less dramatic in its influence. Thus, we obtain a uranyl bond contraction of 0.008 and 0.004 Å for structures **I** and **V**, respectively. The influence on the U−OH bond length is much smaller while the O−H bond length is not influenced at all.

A third parameter to consider is the influence of diffuse functions. By adding a set of diffuse functions to the oxygen basis (6-31+G, 6-31+G*, 6-31+G**) we get uranyl bond contractions of up to 0.007 Å, and considerable lengthening of the U−OH bonds by up to 0.03 Å, Tables 9 and 10. The influence on the O−H bond lengths is smaller but not negligible. Adding diffuse functions on the hydrogen atoms as well (6-31++G* basis) is seen to have practically no influence at all on the optimized geometries.

We conclude from the previous discussion that the combination of an uncontracted uranium basis with the 6-31+G* ligand basis set should yield reasonable results. This basis has been adapted in the rest of this study, unless otherwise stated. More comprehensive investigations of basis set effects are certainly possible. However, the cost of using much bigger basis sets will likely become prohibitive for practical applications.

Finally, it should be noted that the uranyl bond angle in **V** varies in the range 122−129° with the different basis sets, Table 10. It is difficult to extract a clear trend for this parameter. The potential energy surface must be very flat with regard to this angle. This is confirmed by the calculated vibrational frequencies for **V**, Table 4. For instance, the lowest energy mode of **V**, calculated at 59 cm^{-1} (6-31+G*/uncontracted basis), contains a O═U═O bending motion.

IC980057A